Biomedicine & Pharmacotherapy 140 (2021) 111744

Contents lists available at ScienceDirect

Biomedicine & Pharmacotherapy

journal homepage: www.elsevier.com/locate/biopha

Original article

Modeling ANXA2-overexpressing circulating tumor cells homing and high throughput screening for metastasis impairment in endometrial carcinomas

Carolina Herrero [a,1], Jose Brea [b,1], Amparo Pérez-Díaz [b], Emiliano Cuadrado [b], Noelia Ferreño [a], Cristian Pablo Moiola [c], Eva Colás [c,d], Antonio Gil-Moreno [c,d], Rafael López-López [a,d], María Isabel Loza [b], Miguel Abal [a,d,*], Lorena Alonso-Alconada [a,**]

[a] Translational Medical Oncology Group (Oncomet), Health Research Institute of Santiago de Compostela (IDIS), University Hospital of Santiago de Compostela (SERGAS), Santiago de Compostela, Spain
[b] Drug Screening Platform/Biofarma Research Group, Centro Singular de Investigación en Medicina Molecular y Enfermedades Crónicas (CIMUS), Universidade de Santiago de Compostela, Santiago de Compostela, Spain
[c] Biomedical Research Group in Gynecology, Vall d'Hebron Research Institute (VHIR), Universitat Autonoma de Barcelona, Barcelona, Spain
[d] Centro de Investigación Biomédica en Red de Cáncer (CIBERONC), Madrid, Spain

ARTICLE INFO

Keywords:
High-risk endometrial cancer patients
Circulating tumor cells
ANXA2
Homing
Micrometastasis
Daunorubicin

Chemical compounds:
Disulfiram (PubChem CID: 3117)
Nocodazole (PubChem CID: 4122)
Paclitaxel (PubChem CID: 36314)
Doxorubicin (PubChem CID: 31703)
Antimycin A (PubChem CID: 14957)
Clofazimine (PubChem CID: 2794)
Mitoxantrone dihydrochloride (PubChem CID: 51082)
Anisomycin (PubChem CID: 253602)
Daunorubicin hydrochloride (PubChem CID: 62770)
Novobiocin sodium salt (PubChem CID: 54726514)

ABSTRACT

Endometrial cancer (EC) is the most common neoplasm of the female reproductive tract in the developed world. Patients usually are diagnosed in early stage having a good prognosis. However, up to 20–25% of patients are diagnosed in advanced stages and have a higher risk of recurrence, making the prognosis worse. Previously studies identified ANXA2 as a predictor of recurrent disease in EC even in low risk patients. Furthermore, Circulating Tumor Cells (CTC) released from the primary tumor into the bloodstream, are plasticity entities responsible of the process of metastasis, becoming into an attractive clinical target. In this work we validated ANXA2 expression in CTC from high-risk EC patients. After that, we modelled *in vitro* and *in vivo* the tumor cell attachment of ANXA2-expressing CTC to the endothelium and the homing for the generation of micrometastasis. ANXA2 overexpression does not provide an advantage in the adhesion process of CTC, but it could be playing an important role in more advanced steps, conferring a greater homing capacity. We also performed a high-throughput screening (HTS) for compounds specifically targeting ANXA2, and selected Daunorubicin as candidate hit. Finally, we validated Daunorubicin in a 3D transendothelial migration system and also in a *in vivo* model of advanced EC, demonstrating the ability of Daunorubicin to inhibit the proliferation of ANXA2-overexpressing tumor cells.

Abbreviations: EC, endometrial cancer; ER, estrogen receptor; PR, progesterone receptor; ANXA2, Annexin A2; L1CAM, L1 cell adhesion molecule; CTC, circulating tumor cells; ENITEC, European Network for Individualized Treatment in EC; EVs, extracellular vesicles; EMT, epithelial to mesenchymal transition; MET, mesenchymal to epithelial transition; HTS, high-throughput screening; FIGO, International Federation of Gynecology and Obstetrics; EpCAM, epithelial cell adhesion molecule; IK, Ishikawa; H, Hec1A; qPCR, quantitative real time reverse transcription polymerase chain reaction; GAPDH, glyceraldehyde-3- phosphate dehydrogenase; IP, intraperitoneally; DMSO, dimethyl sulfoxide.

* Corresponding author at: Translational Medical Oncology Group (Oncomet), Health Research Institute of Santiago de Compostela (IDIS), University Hospital of Santiago de Compostela (SERGAS), Trav. Choupana S/n, 15706 Santiago de Compostela, Spain.
** Corresponding author.
E-mail addresses: miguel.abal.posada@sergas.es (M. Abal), lorena.alonso@nasasbiotech.com (L. Alonso-Alconada).
[1] Co-first authors with equal contributions.

https://doi.org/10.1016/j.biopha.2021.111744
Received 1 March 2021; Received in revised form 11 May 2021; Accepted 13 May 2021
Available online 25 May 2021

1. Introduction

Endometrial cancer (EC) is the most common gynaecological cancer in developed countries. The majority of cases are diagnosed at early stage, mainly due to symptomatic abnormal uterine bleeding, with a favorable five-year survival rate of over 95%, but this rate drastically drops when there exists regional spread (69%) or distant disease (16%) [1]. Approximately 2–15% of women diagnosed with early stage EC will present recurrent disease, but this recurrence rate increases up to 50% at advanced stages and aggressive histologic conditions [2]. Surgery represents the primary treatment, involving removal of the uterus, fallopian tube and ovaries and surgical staging with lymphadenectomy based on stage, myometrial invasion, and histological grade; in addition, patients with high risk of recurrence receive adjuvant radiotherapy. Chemotherapy, including platinum compounds and taxanes, is restricted to metastatic/recurrent disease and advanced stages or high-risk histological types such as serous [3]. However, traditional chemotherapy regimens are less effective in comparison with cancers of other organs due to resistance to chemotherapy acquired by cancer cells, the non-selectivity of current treatments and the biologic heterogeneity of EC [4–6]. Several immunohistochemical markers have been studied for the prediction of recurrences, like reduced expression of the estrogen receptor (ER) or progesterone receptor (PR), or the enhanced expression of the L1 cell adhesion molecule (L1CAM), described as predictor for distant recurrence and overall survival in EC [7,8], but none of them have been implemented into clinical practice due to limited sensitivity and/or specificity. All this emphasizes the importance of improving the management of advanced disease in EC by identifying new molecular targets and biomarkers associated with a high risk of recurrence and/or with response to therapy. To this regard, we have previously identified and validated Annexin A2 (ANXA2) in a retrospective study including 93 patients showing ANXA2 effectively predicting those endometrioid endometrial carcinomas that finally recurred [9]. Importantly, ANXA2 demonstrated a predictive value also among low risk Stage I endometrioid endometrial carcinomas, highlighting the clinical utility of ANXA2 biomarker as predictor of recurrent disease in EC. We have further extended these findings by demonstrating ANXA2 levels in circulating extracellular vesicles (EVs) being associated with high risk of recurrence and non-endometrioid histology [10].

In parallel, enumeration and molecular characterization of circulating tumor cells (CTC) represent a promising clinical tool for the real-time monitoring of patients under treatment, as one of the liquid biopsy solutions allowing personalized medicine [11]. The quantification of CTC has been demonstrated as independent prognostic factor in advanced breast [12,13], prostate [14] and colorectal cancer [15]. Of interest, the evolution of CTC enumeration during treatment correlate with response to therapy and improved survival [16]. In EC, the findings consistently point to a small percentage of high-risk EC patients presenting with EpCAM positive CTC in circulation at the time of diagnosis, although limited cohort studies have been conducted [17]. The ENITEC (European Network for Individualized Treatment in EC) Consortium described a 22% (n = 32) CTC-positive high-risk EC patients, and characterized these CTC with a plasticity phenotype associated with high-risk of recurrence [18].

In addition to the clinical value of CTC as diagnostic and prognostic biomarker in advanced disease, from a biological perspective CTC that originate from the primary lesion or the existing loco-regional or distant secondary lesions are considered responsible for the generation of new tumor metastasis and an attractive pharmacological target for the impairment of the process of metastasis. The molecular characterization of the CTC also allows to understand better the biology of metastasis and resistance to established therapies [19]. Recent discoveries describing the stepwise process of metastasis interpret these CTC as highly plasticity entities that must efficiently attach to preferred sites that will colonize and result in micrometastasis [20–22]. The epithelial to mesenchymal transition (EMT), resulting in the downregulation of epithelial markers and the acquisition of mesenchymal properties, increases the capacity of tumor cells to migrate and invade the surroundings and favors their intravasation into the blood stream, and the reverse process, the mesenchymal to epithelial transition (MET), would allow CTC to attach at preferred tissues generating micrometastasis [23,24]. An association between CTC and ANXA2 has been described in early breast cancer, related to EMT [25]. Based on these premises, we aimed to develop a novel therapeutic strategy in EC that might impair CTC attachment at these pre-metastatic niches. For this, we (i) validated ANXA2 expression in CTC from high-risk endometrial cancer patients, (ii) modelled CTC in circulation and homing, (iii) performed a high-throughput screening (HTS) for compounds specifically targeting ANXA2, and (iv) validated the potential candidates in appropriate *in vitro* and *in vivo* models of advanced endometrial cancer.

2. Materials and methods

2.1. Patients

A total of 57 endometrial cancer patients with high-risk of recurrence were recruited at three hospitals in Spain (University Clinical Hospital of Santiago de Compostela, Vall d'Hebron University Hospital and MD Anderson Cancer Center Madrid). All patients signed the informed consent approved by the ethical committee (RLL-ANT-2014-01; 17 October 2014; Rede Galega de Comités de Ética da Investigación). Inclusion criteria for participation in the study were patient with high-risk of recurrence: FIGO stage III or IV endometrioid endometrial carcinomas, Grade 3 carcinomas, >50% myometrial invasion, clear cell or serous carcinomas (Supplementary Table 1).

2.2. ANXA2 expression in CTC from high-risk endometrial cancer patients

CTC were isolated based on the expression of epithelial cell adhesion molecule (EpCAM) using the CELLection^{TM} Epithelial Enrich kit (Invitrogen, Dynal, Oslo, Norway), as described [18]. ANXA2 expression in CTC was determined by qPCR upon total RNA extraction with the QIAmp viral RNA mini kit (Qiagen, Valencia, CA). cDNA was synthesized using SuperScriptIII (Invitrogen, Carlsbad, CA, USA) according to the user's guide. ANXA2 and CD45 genes were pre-amplified using TaqMan PreAmp Master Mix kit (Applied Biosystems, Foster City, CA) with 14 reaction cycles. qPCR was carried out using TaqMan Gene Expression Master Mix kit (Applied Biosystems, Foster City, CA) and a 7.500 quantitative Real-time PCR Machine. Data were analyzed with StepOne Software v.2.1 (Applied Biosystems, Foster City, CA) and normalized to protein tyrosine phosphatase receptor type C (PTPRC, CD45), as a previously validated marker of non-specific isolation [26]. Data are represented as the Cq value of ANXA2 normalized to 40 (maximum number of cycles) ($40 - Cq_{ANXA2}$), and this value was normalized to the 40-Cq_{CD45} ($(40 - Cq_{ANXA2}) - (40\text{-}Cq_{CD45})$).

2.3. Data evaluation and statistical analysis

The median value of ANXA2 expression in the CTC population of endometrial cancer patients was defined as the cutoff to classify the patients as Low or High ANXA2 CTC levels. Kaplan-Meier with log-rank test were used to determine progression-free survival and overall survival curves.

2.4. Cell lines

2.4.1. Endometrial cancer cell lines

Human EC cell lines Ishikawa (IK; HPA Culture Collections) and Hec1A (H; ATCC), were maintained in DMEM-F12 (Gibco, Grand Island, NY, USA) and McCoy's 5A medium (Gibco, Grand Island, NY, USA), respectively, supplemented with 10% FBS and 1% penicillin-

streptomycin at 37 °C in 5% CO_2. Both cell lines were previously infected with luciferase expressing pLenti CMV V5-LUC Blast (w567-1) (Addgene, Cambridge, MA) vector in the presence of polybrene (8 μg/ml; Sigma, St. Louis, MO, USA). The pmCherry-N1 (Clontech Laboratories, CA, USA) empty vector (Supplementary Fig. 1A) or the construction for ANXA2 gene overexpression were transfected using Lipofectamine 2000 (Invitrogen, Carlsbad, CA, USA), to obtain IK-Ctrl and H-Ctrl or IK-ANXA2 and H-ANXA2 cells, respectively. Cells were selected using geneticin (0.5 mg/ml, Sigma, St. Louis, MO, USA) and blasticidine S HCl (3 mg/ml, Invitrogen, Carlsbad, CA, USA).

IK cells infected with lentiviral particles containing the empty vector (pLKO.1-puro; Sigma, MO) to obtain IK-pLKO cells or the ANXA2 shRNA vector (5'-CC GGCCTGCTTTCAACTGAATTGTTCTCGAGAACAATTCA GTTGAAAGCAGGTTTTTG-3'; Sigma Mission NM_001002857, Sigma, MO, USA) to stably silence ANXA2 expression (IK-shANXA2) were previously characterized [9] and were used for the High Throughput Screening assay.

2.4.2. Endothelial cell line

EAhy926 human endothelial cell line (ATCC) was maintained in DMEM medium supplemented with 10% FBS and 1% penicillin-streptomycin at 37 °C in 5% CO_2. EAhy926 cells were infected with lentiviral particles with the GFP reporter gene (MISSION® TurboGFP™ Control Vector; Sigma, MO, USA), in the presence of polybrene (8 μg/ml; Sigma, St. Louis, MO, USA), to obtain EAhy926-GFP cells, and selected with puromycin (0.5 μg/ml Sigma, MO, USA).

2.5. RNA isolation and real-time quantitative PCR (qPCR)

Total RNA was isolated from IK-Ctrl, IK-ANXA2, H-Ctrl and H-ANXA2 cells using High Pure RNA Isolation Kit (Roche, Applied Science, Indianapolis, IN) and cDNA synthesis was carried out using MuLV reverse transcriptase (Applied Biosystems, Foster City, CA), according to the manufacturer. qPCR was performed using TaqMan assays (ANXA2#Hs01561520_m1; GAPDH#Hs99999905_m1; Applied Biosystem, Foster City, CA) in a 7500 Real-Time PCR Machine. Data were analyzed with StepOne Software v.2.1 (Applied Biosystems, Foster City, CA). The results were represented as the fold change in gene expression relative to Glyceraldehyde-3-phosphate dehydrogenase (GAPDH) gene expression ($2^{-\Delta\Delta Cq}$). Values were expressed as Mean±SEM from at least three independent experiments in triplicate.

2.6. Western blot

IK-Ctrl and IK-ANXA2 cells were washed with PBS and lysed in lysis buffer [0.1% SDS, 150 mM NaCl, 50 mM Tris-HCl (pH 8.5), 0.5% DOC, 1% NP-40, 2 mM Na3VO4, 4 mM NaF, 13 PIC]. 30 μg of the cell lysates were resolved by 12% SDS-PAGE and transferred to a PVDF membrane (Amersham Bio- science, Buckinghamshire, UK). After blocking, the membrane was incubated with anti-ANXA2 (1:500 dilution; Abcam, Cambridge, UK), anti-Vimentin (1:1000 dilution; Dako, Sant Just Desvern, Barcelona) or b-Actin (1:1000; Abcam, Cambridge, UK) antibodies, overnight at 4 °C followed by each corresponding secondary antibody at room temperature for 1 h. Immobilon Western Blotting Kit (Millipore, Billerica, MA) was used to detect protein signal.

2.7. Transwell migration assay

24-well transwell plate (8.0 μm pore size polycarbonate membrane; Corning, NY, USA) was used as previously described [9] Briefly, 5×10^4 cells were seeded on the upper side of the transwell in 200 μl of serum-free DMEM F-12 medium. The lower side of the chamber was filled with DMEM F-12 supplemented with 10% FBS, to form a gradient. After incubation at 37ºC for 48 h, migrated cells were trypsinized, collected, stained with 4 μM/l calcein acetoxymethyl ester (Invitrogen, Paisley, UK) and visualized at 485 nm using a fluorimeter. Results were presented as relative percentage of migrated cells respect to IK-Ctrl cells, defined as 100%. Values were expressed as Mean±SEM from at least three independent experiments in triplicate.

2.8. Tumor cells adhesion to the endothelium

4×10^5 EAhy926-GFP cells were seeded in a commercial system of parallel channels (μ-Slide $VI^{0.4}$ ibiTreat, Ibidi GmbH, Grafelfing, Germany), mimicking the creation of an artificial blood vessel. 10^6 cells/ml IK-Ctrl and IK-ANXA2 tumor cells or H-Ctrl and H-ANXA2 cells were previously DiD dyed (Vybrant™ DiD Cell-Labeling Solution, Thermofisher, MA, USA), according to the manufacturer. Once the monolayer of endothelial cells was formed, each tumoral cell line was recirculated in a different channel for 2 h using a perfusion pump (Tubing pump, REGLO digital, ISMATEC®, Wertheim, Germany). Adherent cells were observed using a fluorescence microscopy (Zeiss, Axio Vert. A1, Jena, Germany) and the fluorescence was quantified using the ImageJ program. Values were expressed as Mean±SEM from at least three independent experiments in triplicate.

2.9. Modeling circulating tumor cells homing

A 35 mm Petri dish (μ-$Dish^{35\ mm,\ high}$ ibiTreat, Ibidi GmbH, Grafelfing, Germany) and a silicone tube (Cole-Parmer Instrument Company, Illinois, USA) were used to perform an artificial blood vessel through the dish. The tube was placed inside the dish, and then was filled with 1.8% agarose (Agarose Low Melting Point Analytical, Promega, Wisconsin, USA) and polymerized during 1 h at 4 °C. After polymerization, the tube was removed to create a hollow channel through the dish and 100 μl of 2% Laminin (Laminin from Engelbreth-Holm-Swarm murine sarcoma, Sigma, MO, USA) was injected through the channel. 2×10^6 H-Ctrl or H-ANXA2 cells were DiD or DiO (Vybrant™ DiO Cell-Labeling Solution, Thermofisher,MA,USA) dyed, respectively, according to the manufacturer. Tumor cells were recirculated for 1 h using a Tubing perfusion pump. The system was cleaned using McCoy's 5a Medium Modified (Gibco, Grand Island, NY, USA) to remove unattached tumoral cells. The dish was maintained at 37 °C in 5% CO_2, recirculating McCoy's 5a Medium Modified overnight.

Images from different areas of the channel were taken at 24 h and 4 days using a fluorescence microscopy (Zeiss, Axio Vert. A1, Jena, Germany) and the fluorescence was quantified using the ImageJ program. Values were expressed as Mean±SEM. from at least three independent experiments in triplicate.

2.10. Primary screening: IK-pLKO cell viability

Prestwick Chemical Library® composed by a collection of 1120 small molecules was tested during a primary screening. The ability of the compounds to inhibit IK-pLKO cells proliferation in an anchorage independent colony formation assay, was evaluated. Briefly, 50 μl of 0.6% low melting point agarose (Promega, Wisconsin, USA) solution containing 10% FBS was used to overlaid the bottom of 96-well plates. 100 μl of 0.3% agarose solution containing 10% FBS and 4×10^3 IK-pLKO cells were added per well using a multichannel micropipette. Next day, 50 μl of DMEM F-12 or the 1120 different compounds (final concentration of 10^{-5} M in culture medium) were added using a multichannel micropipette. After 5 days of incubation at 37 °C with 5% CO_2 colonies were stained with Alamar Blue (Invitrogen, Carlsbad, CA), according to the manufacturer, and the fluorescence was measured at an excitation wavelength of 531 nm and an emission wavelength of 590 nm.

Positive (cells without treatment) and negative (cells treated with Docetaxel 1.2 μM) controls were included in all plates, as well as points with the reference compound at a concentration equivalent to its IC_{50} (17 nM).

In a confirmatory screening 34 compounds selected from the primary

screen were re-assayed in three different experiments and finally 27 compounds were considered as confirmed hits. Validated hits were defined as those compounds that inhibited the IK-pLKO cells proliferation with at least an IC_{50} ten times lower than the one for IK-shANXA2 cells.

Dose-response curves were calculated using GraphPad Prism 4.00 software (GraphPad Software, San Diego, CA) to determine the IC_{50} values for each cell line. Values were expressed as Mean±SEM from at least three independent experiments in triplicate.

2.11. 3D transendothelial migration assay

A clear bottom 96-well plate (Perkin Elmer, MA, USA) was covered with 3D Culture Matrix™ Rat Collagen I (Cultrex, Abingdon, UK), using 7.5% (w/v) Sodium Bicarbonate for neutralization, and culture medium to a final concentration of 1.6 mg/ml. The plate was centrifuged for 10 min at 300×*g* and 4 °C. After 45 min polymerization at 37° in 5% CO_2, a RAFT absorber plate (TAP Biosystems, Wilmington, USA) was placed on top of the collagen to absorb the medium for 15 min. The collagen layer was then treated with 2% Laminin (Laminin from Engelbreth-Holm-Swarm murine sarcoma, Sigma, MO, USA) for 30 min and 6×10^4 EAhy926-GFP cells were seeded on top of the layer. The next day, 12×10^3 cells IK-ANXA2 cells, previously dyed with DiD (Vybrant™ DiD Cell-Labeling Solution, Thermofisher, MA, USA), according to the manufacturer, were seed in the presence or not of Daunorubicin at 10^{-7} M, 3×10^{-7} M and10^{-6}M.

At baseline and seven days after incubation at 37ºC in 5% CO_2, four fields in each individual well were automated imaged using the Operetta® High Content Imaging System (PerkinElmer, MA, USA), taken planes every 5 μm. Excitation: 460–490 nm, emission: 500–550 nm to measure GFP and excitation 620–640 nm emission 660–760 nm to measure DiD. Images were analyzed using ImageJ program. Values were expressed as Mean ± SEM from at least three independent experiments.

2.12. Mice model of endometrial cancer recurrence

For experimental *in vivo* assay, 20 female CB17-SCID CD-17/lcr/Prkdc scid/Rj mice aged 28 weeks (Janvier Labs, Le Genest-Saint-Isle, France) were divided in four groups and inoculated with 2×10^6 H-Ctrl or H-ANXA2 endometrial cancer cells, intraperitoneally (IP). At the time of injection, the control group received placebo (saline solution with DMSO) *via* intraperitoneal injection and the treated group received Daunorubicin IP (1 mg/kg in saline solution). Daunorubicin hydrochloride was purchased from Sigma (ref. 30450) and dissolved in DMSO. The treatment was repeated on day 5. Tumor metastasis were detected by bioluminescent imaging with a Xenogen IVIS (Xenogen, Caliper Life Sciences, PerkinElmer, Waltham, MA) system coupled to Living Imaging software 4.2 (Xenogen Corporation) at day 6. Luciferin (150 mg/kg in PBS; Firefly Luciferin, Caliper Lifescience Corp, Hopkinton, MA) was injected IP as the substrate for the luciferase. Mice were housed and maintained under specific pathogen-free conditions. All animal experiments were carried out in accordance with the EU Directive 2010/63/EU for animal experiments and approved by the Use Committee for Animal Care from University of Santiago de Compostela (USC).

3. Results

3.1. Validation of ANXA2 expression in CTC from high-risk of recurrence endometrial cancer patients

The expression of ANXA2 in EC patients was analyzed by qPCR in purified circulating tumor cells (CTC). Briefly, EpCAM-based immunoisolation was used to purify CTC from peripheral blood from EC patients at high-risk of recurrence (n = 57; see Supplementary Table 1 for clinical variables of the cohort included in this study). DNA was extracted and processed as described [18], and the expression levels of ANXA2 in CTC relative to the background of unspecific non-tumor cell isolation were used to evaluate the correlation of CTC load with progression-free survival (PFS) and overall survival (OS). As shown, patients with high ANXA2 expression levels in CTC were associated with shorter time to progression, with a mean of 34.85 months, whereas in those patients with low levels of ANXA2, PFS times increased up to 45.52 months (Fig. 1A; $p = 0.108$;). Overall survival was also decreased in patients with high ANXA2 expression levels in CTC (Fig. 1B; $p = 0.208$). These results confirmed the clinical utility of CTC monitoring in advanced EC [18], and the value of ANXA2 for the stratification of patients [9].

3.2. ANXA2 overexpression on EC cell lines promotes a mesenchymal phenotype

Once clinically validated, we next explored the impact of ANXA2 expression on the fate of CTC during circulation in blood and homing at sites of future metastasis. For this, we modelled *in vitro* and *in vivo* the sequential steps of tumor cell attachment and extravasation, and initially recreated endometrial CTC by increasing ANXA2 expression in the Ishikawa (IK-ANXA2; Fig. 1C) and Hec1A (H-ANXA2; Supplementary Fig. 1B) human EC cell lines. Of note, the enhanced ANXA2 expression resulted in a transition from an epithelial to a more mesenchymal phenotype, characterized by an increased Vimentin expression (Fig. 1C; $^{**}p = 0.002$ (Supplementary Fig. 1B) and Fig. 1D (Supplementary Fig. 1C)), and a cell migratory promotion as analyzed by transwell migration assay after 48 h of incubation compared to control Ishikawa cells (Fig. 1E; $p = 0.062$). These evidences are in agreement with previous results, proposing an association of endometrial cancer CTC with a metastasis-supporter plasticity phenotype [18].

3.2.1. ANXA2 overexpression on CTC promotes metastasis process

To model *in vitro* the stepwise process that CTC must accomplish once incorporated into the circulation, including the efficient attachment to the endothelium and the homing for the generation of micrometastasis, we set up microfluidic systems to perfuse EC tumor cells within simulated endothelial vessels (scheme in Fig. 2A, upper panel). We first analyzed the impact of ANXA2-expression in EC CTC that eventually contact an endothelium to generate a cell-cell interaction that may result in tumor cell homing. For this, a monolayer of green fluorescent protein-expressing human endothelial cells (EAhy926-GFP) were seeded coating the perfusion channels and individualized Cherry-expressing EC tumor cells were physiologically perfused on a humidified atmosphere at 37ºC and 5% CO_2 for two hours. After perfusion, ANXA2-overexpressing Ishikawa cells (IK-ANXA2) adhered to the endothelium were quantified by fluorescent imaging, showing an endothelial adhesion efficiency similar to that of control Ishikawa cells (Fig. 2A, histogram; $p = 0.222$). Similar results, with no significant differences between control (H-Ctrl) and ANXA2-overexpressing (H-ANXA2), were observed with Hec1A cells (Fig. 2A, histogram, $p = 0.474$). This is in accordance with the mesenchymal phenotype characterizing endometrial CTC resulting in a limited efficiency to establish focal contacts with endothelial cells [27], but in apparent contradiction of a more aggressive tumor cell line.

We thus improved the complexity of the model system by integrating the dynamic homing of CTC (scheme in Fig. 2B). We incorporated a polymerized agarose matrix as the basement for CTC homing to the microfluidic system, and performed a competitive tumor cell attachment assay with DiD dyed control Hec1A EC cell line (H-Ctrl red tagged cells in Fig. 2B), that showed a more competent cell attachment performance compared to Ishikawa cells (see Fig. 2A), and DiO dyed ANXA2-overexpressing Hec1A EC cell line (H-ANXA2; green tagged cells in Fig. 2B). Individualized cells were perfused for an hour and further incubated for up to four days to study the next step of tumor cell homing upon attachment to the endothelium. As above, Hec1A cells overexpressing ANXA2 demonstrated less efficiency at initial attachment to

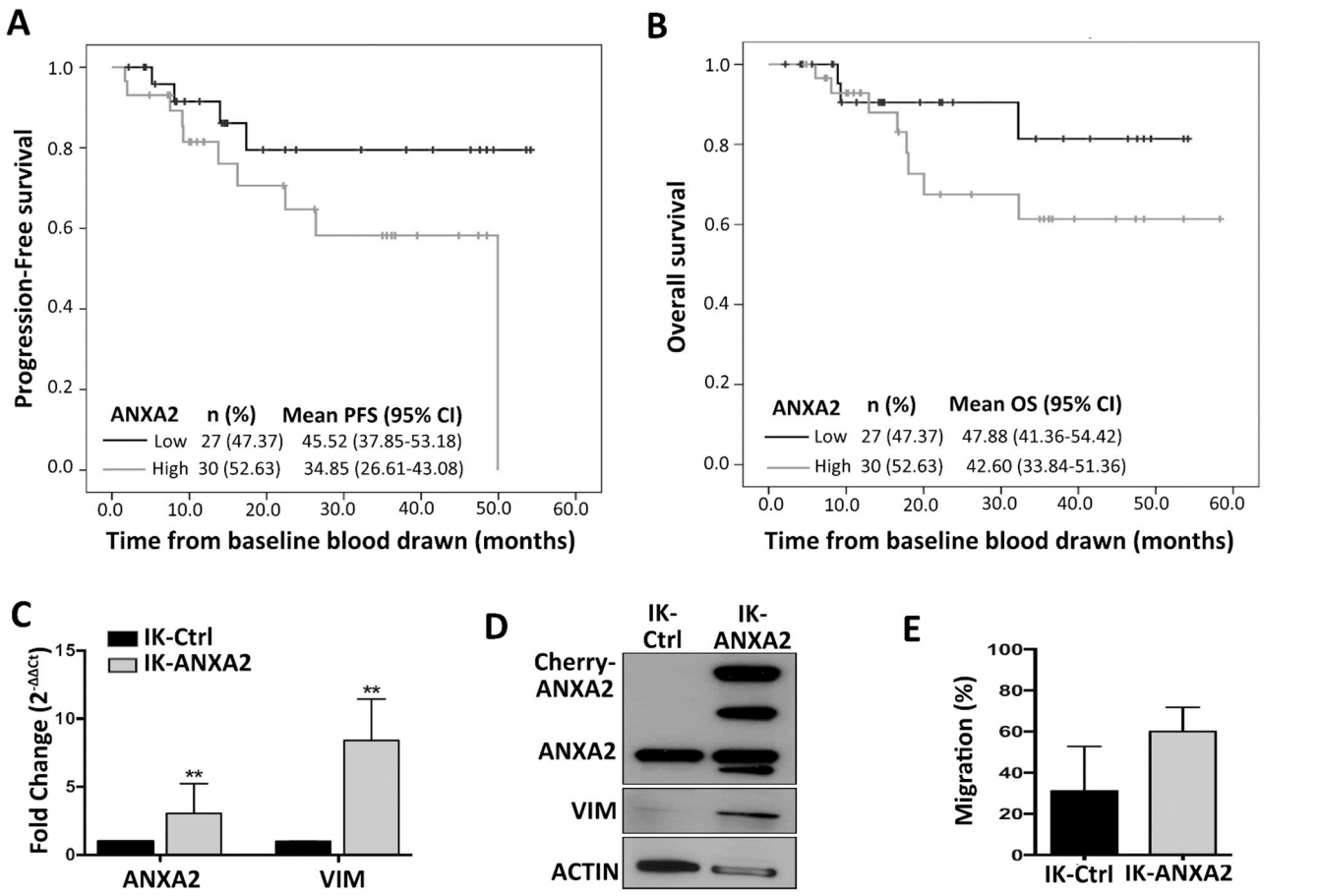

Fig. 1. Analysis of ANXA2 expression in CTC from endometrial cancer patients at high-risk of recurrence and IK endometrial cancer cells characterization. Kaplan-Meier survival curves among 57 endometrial cancer patients stratified by ANXA2 expression levels in CTC. (A) Progression-free survival (Long-rank test; $p = 0.108$) and (B) Overall survival curves (Long-rank test, $p = 0.208$). (C) Overexpression of ANXA2 in IK cell line raised VIM in mRNA level (Mean±SEM; Mann-Whitney test; $^{**}p = 0.002$) and (D) protein level. (E) Effect of IK cell line ANXA2 overexpression on transwell migration assays (Mean ± SEM; Mann-Whitney test; $p = 0.062$).

the endothelial monolayer, resulting in a reduced percentage of these aggressive tumor cells at 24 h after circulation as quantified by fluorescence imaging (Fig. 2B; histogram; t = 24 h). More interestingly, after four days of incubation ANXA2-overexpressing Hec1A cells showed a more competent micrometastasis formation as quantified by fluorescence imaging (Fig. 2B; histogram; t = 4 days). Overall, these results suggested that ANXA2 expression in endometrial CTC promotes the transition to a more mesenchymal phenotype associated with improved invasive capabilities but limited adhesion properties consistent with CTC plasticity; this results in a more efficient process of dissemination and homing at distant sites for the generation of micrometastasis in targeted organs.

We finally analyzed the impact of ANXA2 overexpression in a preclinical *in vivo* model of endometrial cancer dissemination. Endometrial metastatic cells present both hematogeneous and peritoneal dissemination, resulting in loco-regional and distant recurrences. We thus modelled CTC attachment to a mesothelium by injecting luciferase-expressing Hec1A cells with or without ANXA2 enhanced expression, in the peritoneal cavity of immunodeficient mice (scheme in Fig. 2C). After injection, the efficiency of Hec1A cell attachment was evaluated by bioluminescence with no significant differences between groups at t = 0 h (t = 0 h in Fig. 2C; upper histogram; n = 5; $p = 0.413$), in accordance with *in vitro* results. By contrast, bioluminescence signal was significantly enhanced in those animals injected with ANXA2-overexpressing Hec1A cells at six days after tumor cell injection (t = 6 days in Fig. 2C; lower histogram; n = 5; $^{**}p = 0.008$), indicative of an improved capability to generate peritoneal micrometastasis, and also consistent with the invasive properties that favours homing in dynamic conditions shown *in vitro*. In addition to validate the metastatic potential of EC cells with enhanced expression of ANXA2, these results support the potential of ANXA2 as an attractive target for the impairment of CTC homing and metastasis.

3.3. High-throughput screening (HTS) for compounds specifically targeting ANXA2

To identify compounds specifically targeting ANXA2, we performed a high-throughput screening (HTS) with the Prestwick Chemical Library (PCL) collection of 1120 compounds comprising mostly approved off-patent drugs (FDA, EMEA and other agencies) selected for their high chemical and pharmacological diversity, with known bioavailability and safety data in humans. The workflow to conduct the HTS was as follows (Fig. 3A, lower panel): in a first screening, we evaluated the efficacy of the compounds to inhibit the proliferation of control Ishikawa cell line (IK-pLKO) in a 3D colony formation assay that mimics the formation of micrometastasis. Briefly, control Ishikawa cells were seeded in 96-well plates on top of a 0.6% low melting point agarose coating, embedded onto a 0.3% agarose layer (see scheme in Fig. 3A), and incubated with each of the 1120 PCL compounds at 10^{-5} M concentration for five days, as described in Materials and Methods. The threshold for identifying active compounds was fixed to the standard criteria of a percentage of inhibition higher than the mean+ 3 *standard deviation of the whole chemical library, being fixed at a 60% inhibition of IK-pLKO colony growth compared to control culture media (Fig. 3B). With this criteria,

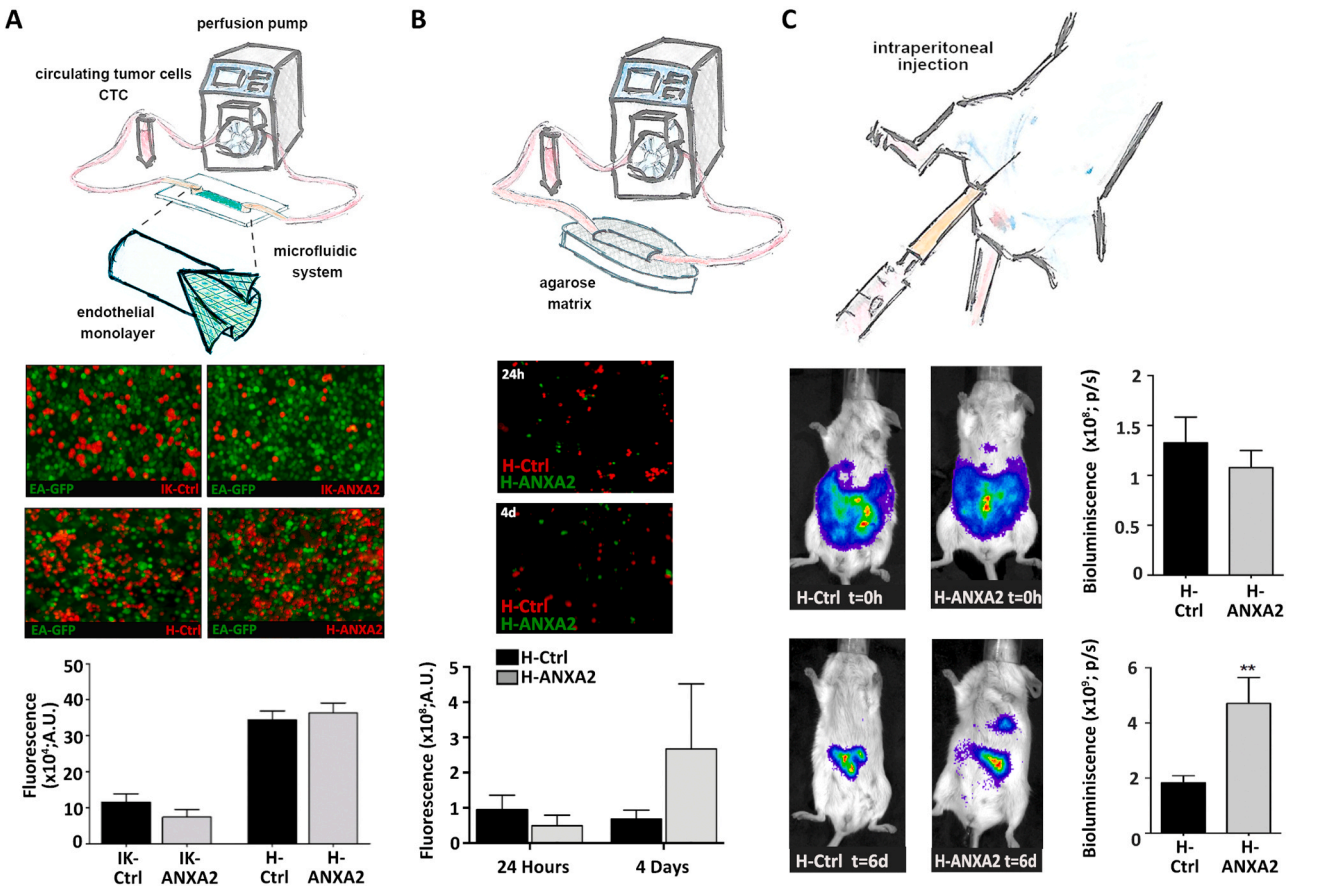

Fig. 2. Effect of ANXA2 overexpression on endometrial cancer cells adhesion and micrometastasis formation. (A) Schematic image of adhesion assay (upper panel). Representatives images of IK and Hec1A cancer cells stained with DiD (red) adhered to an EAhy926-GFP endothelial cells (green) monolayer in a commercial system of parallel channels (middle panel). Magnification x10. Quantification of the total area of fluorescent adhered cells (Histogram; Mean ± SEM; Mann-Whitney test; IK cells $p = 0.222$ and Hec1A cells $p = 0.474$). (B) Schematic image of agarose micrometasis formation assay (upper panel). Representative images of H-Ctrl (DiD stained, red) and H-ANXA2 (DiO stained, green) cells 24 h (upper middle panel) and 4 days (lower middle panel) after perfusion. Quantitative data of the total area of H-Ctrl and H-ANXA2 fluorescence 24 h and 4 days after perfusion (Histogram; Mean ± SEM; Kruskal-Wallis test; p = ns). (C) Schematic image of intraperitoneal mice mode (upper panel). IVIS bioluminescence images of an *in vivo* peritoneal metastasis assay after injection (t = 0 h; middle panel) and 6 days after intraperitoneal injection of H-Ctrl and H-ANXA2 EC cells (t = 6d; lower panel). Quantification of bioluminescence images (Histogram; Mean ± SEM; Mann-Whitney test; $p = 0.413$ and $^{**}p = 0.008$, respectively) (For interpretation of the references to color in this figure legend, the reader is referred to the web version of this article).

thirty-four (34) potential inhibitory compounds were identified, being twenty-seven (27) hits confirmed in an independent assay. These 27 confirmed hits were assayed in a secondary screening based on 3D colony formation comparison between control IK-pLKO cells and Ishikawa cells with silenced ANXA2 expression (IK-shANXA2). From this screening two validated hits showing IC_{50} values at least 10-fold lower at IK-pLKO *vs* IK-shANXA2 cells were found: Daunorubicin with $IC_{50} = 8.062 \times 10^{-7}$ M and $IC_{50} = 8.421 \times 10^{-6}$ M for IK-pLKO and IK-shANXA2 cells, respectively (Fig. 3C); and Novobiocin, with $IC_{50} = 1.310 \times 10^{-7}$ M and $IC_{50} = 2.004 \times 10^{-6}$ M in IK-pLKO and IK-shANXA2 cells, respectively (Supplementary Fig. 2A). The *in vitro* micrometastasis inhibitory efficacy of these two compounds were interrogated with the ANXA2-overexpressing Ishikawa cell line, confirming the specific targeting of ANXA2 with Daunorubicin with an $IC_{50} = 4.765 \times 10^{-7}$ M and $IC_{50} = 6.884 \times 10^{-8}$ M in IK-Ctrl and IK-ANXA2 cell lines, respectively (Fig. 3D). By contrast, Novobiocin was not validated with an $IC_{50} = 1.589 \times 10^{-6}$ M and $IC_{50} = 2.888 \times 10^{-6}$ M in IK-Ctrl and in IK-ANXA2 cell lines, respectively (Supplementary Fig. 2B), and was excluded for further validation. Daunorubicin was then selected as candidate hit for *in vitro* and *in vivo* targeting of CTC in EC.

3.4. Validation of Daunorubicin in a 3D transendothelial migration system and in vivo model

To evaluate *in vitro* the efficacy of Daunorubicin in a clinically relevant context that reproduce the interaction of CTC with an endothelial monolayer, we generated a 3D culture system by disposing a compressed high-density collagen layer on top of which GFP-expressing endothelial cells were seeded. Once the endothelial monolayer was formed, DiD dyed IK-ANXA2 tumor cells were added and their attachment and micrometastasis formation was evaluated with time (Fig. 4A). This preclinical *in vitro* model permitted the dynamic evaluation of the endothelial layer disintegration upon CTC attachment and the colonization capabilities of these CTC by real-time analysis with the Operetta® High Content Imaging System, acquiring semi-confocal images at different planes at sequential times. As shown in Fig. 4B, Ishikawa cells overexpressing ANXA2 (IK-ANXA2) were able to attach to and impair the endothelial monolayer before colonizing the underneath collagen basement matrix to generate tumor colonies and micrometastasis. This complete sequence of events recapitulating the attachment and homing of endometrial CTC in circulation were dynamically investigated in the timeframe of seven (7) days. More interestingly, this sequential metastatic colonization was precluded by the addition of Daunorubicin in a concentration-dependent manner, confirming the results described in the HTS targeting ANXA2-expressing cells (Fig. 4C). Of note, the

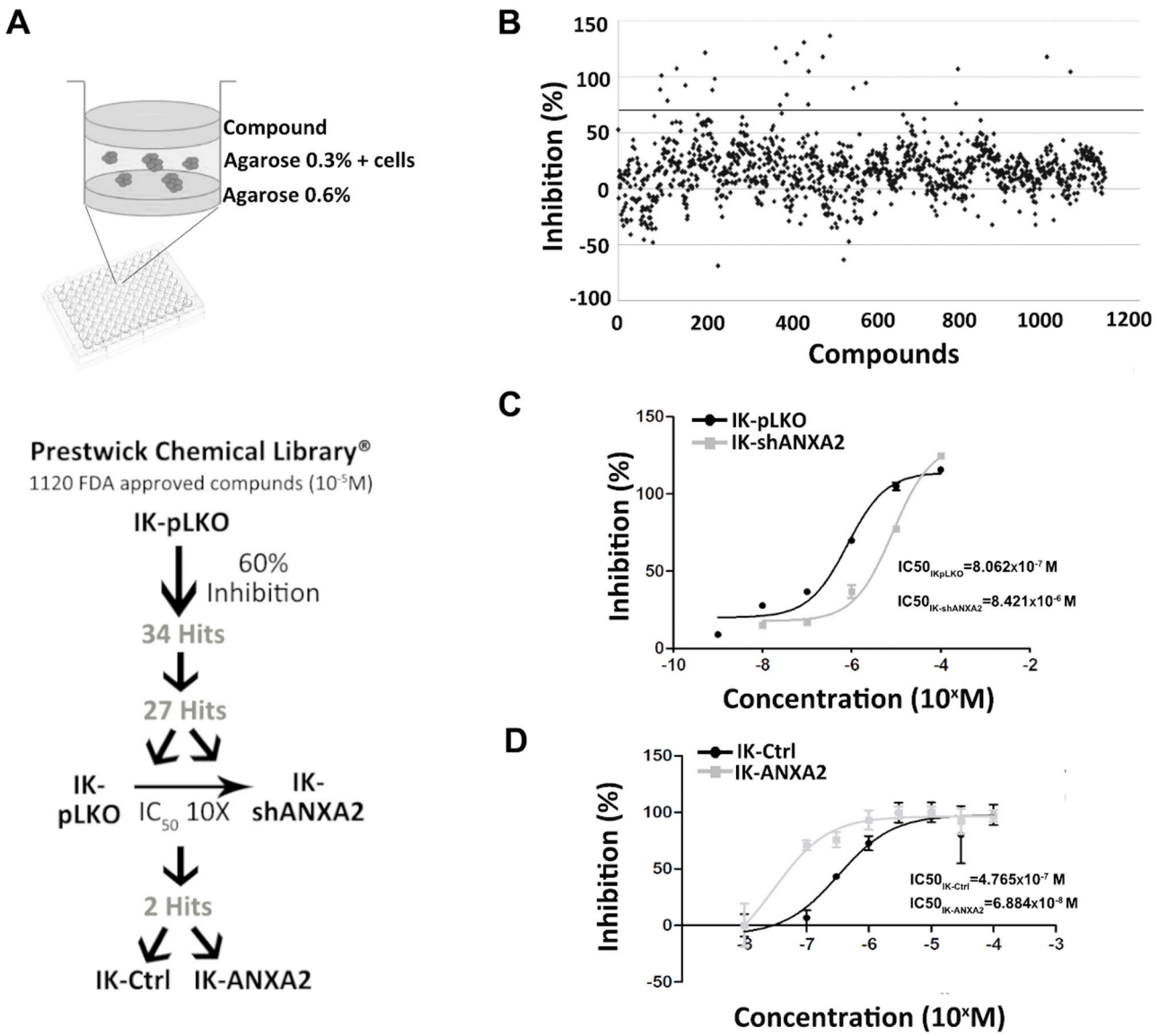

Fig. 3. Identification of ANXA2 inhibitors by *high throughput screening* (*HTS*) in a 96 well plate colony formation assay. (A) Schematic image of *HTS* assay (upper panel) and workflow design for *HTS* (lower panel). (B) Proliferation inhibition rate (>60%). (C) Dose-response curves comparing the cytotoxic activity of Daunorubicin in IK-pLKO ($IC_{50} = 8062 \times 10^{-7}$ M) and IK-shANXA2 ($IC_{50} = 8421 \times 10^{-6}$ M) cells and (D) in IK-Ctrl ($IC_{50} = 4765 \times 10^{-7}$ M) and IK-ANXA2 ($IC_{50} = 6884 \times 10^{-8}$ M) cells for 5 days.

impairment of CTC attachment and further colonization occurred without altering the integrity of the endothelial monolayer further indicating that Daunorubicin acted specifically on the ANXA2-expressing tumor cells while not affecting normal endothelial cells (Supplementary Fig. 3).

We finally assessed the ability of Daunorubicin to impair *in vivo* the attachment of CTC to the peritoneal mesothelium and to avoid loco-regional metastasis by using the preclinical model of intraperitoneal injection of Hec1A EC cells. The efficiency of control Hec1A cells with basal levels of ANXA2 compared to that of Hec1A cells over-expressing ANXA2 (H-ANXA2) to generate tumor implants under Daunorubicin treatment was analyzed by bioluminescence at six (6) days after peritoneal injection of tumor cells (Fig. 4D). Daunorubicin (1 mg/kg) was administered intraperitoneally at day 0 and day 5, and total bioluminescence signal was quantified by live imaging upon injection of luciferin substrate using the Xenogen IVIS system. Daunorubicin demonstrated an improved ability to inhibit tumor cell proliferation depending on ANXA2 expression, in this preclinical model of peritoneal dissemination of advanced EC. As shown, the pattern of peritoneal metastasis was drastically reduced in those mice injected with the ANXA2 over-expressing Hec1A cells upon Daunorubicin treatment (Fig. 4D), further confirmed by the quantification of bioluminescence signal from the peritoneal metastatic implants (Fig. 4E). All these results reinforce the validity of a therapeutic strategy specifically targeting the population of disseminating tumor cells responsible of metastasis. They also confirm the potential of Daunorubicin for the inhibition of tumor cell adhesion associated with the plasticity phenotype resulting from the enhanced expression of ANXA2, for the prevention of recurrent disease in EC.

4. Discussion

The acquisition of a mesenchymal phenotype is associated with cell migratory and invasive properties that might be translated into the resulting circulating tumor cells (CTC). This plasticity phenotype can be detected in CTC immunoisolated from endometrial cancer (EC) patients with high-risk of recurrence [18], with mesenchymal traits participating in micrometastasis formation [28]. Furthermore, previous studies have

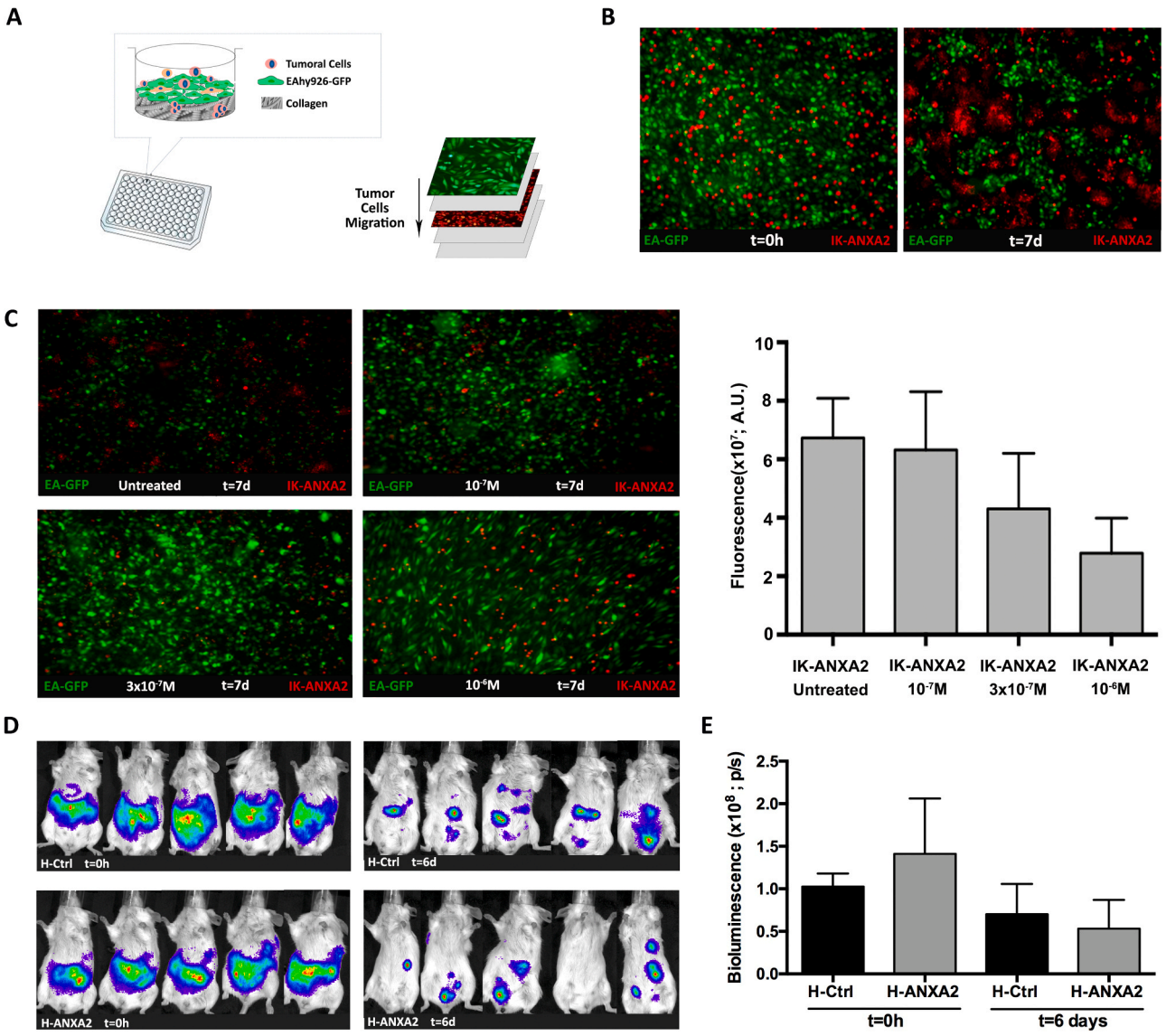

Fig. 4. Validation of Daunorubicin in ANXA2 overexpressing EC cells in 3D transendothelial migration culture using Operetta® High Content Imaging System and in a mice model. (A) Schematic image of the 3D culture assay design. (B) Representative images of EAhy926-GFP endothelial cells (green) and IK-ANXA2 cells (DiD stained, red) at initial time (t = 0 h; left panel) and 7 days (t = 7d; right panel). (C) Representative image of EAhy926-GFP endothelial cells (green) and IK-ANXA2 cells (DiD stained, red) untreated or treated with increasing concentrations of Daunorubicin (10^{-7} M, 3×10^{-7} M,10^{-6} M) for 7 days (left panel). Quantification of the total area of fluorescent IK-ANXA2 cells (Histogram; Mean ± SEM; Kruskal-Wallis test; p = ns). (D) Validation of Daunorubicin in ANXA2 overexpressing Hec1A cells in an intraperitoneal mice model. IVIS bioluminescence images of an *in vivo* peritoneal metastasis assay at initial time (t = 0 h; left panel) and 6 days after intraperitoneal injection of H-Ctrl and H-ANXA2 EC cell lines treated with Daunorubicin (1 mg/kg) (t = 6d; right panel). (E) Quantification of bioluminescence images (Mean ± SEM; Kruskal-Wallis test; p = ns) (For interpretation of the references to color in this figure legend, the reader is referred to the web version of this article).

shown that ANXA2 is involved in the EMT process, contributing to the acquisition of cellular capacities related to the promotion of metastasis, and with clinical utility in primary endometrial carcinomas as a predictor biomarker of recurrent disease [9]. In this new work, we have translated this clinical value to the liquid biopsy context, with a correlation of ANXA2 expression in CTC with progression free survival and overall survival in a cohort of advanced EC patients. The impact of ANXA2 enhanced expression in CTC was associated with a deficient cell adhesion, compensated with a more efficient invasive and colonization capabilities, as demonstrated both *in vitro* and *in vivo* model systems mimicking the clinically relevant events that CTC may accomplish to effectively result in micrometastasis. These clinical and functional validations, indicative of ANXA2 as an attractive molecule to monitor recurrent disease, also suggest that ANXA2 could be further exploited as a target to impair the colonization abilities of endometrial CTC. ANXA2 is a Ca2+-dependent lipid binding protein, member of the annexin family, localized in the nucleus, cytoplasm and extracellular space, and participates in various cellular processes including signal transduction, endocytosis and exocytosis, proliferation, differentiation and apoptosis [29]. ANXA2 plays a relevant role in various types of cancer [30], and enhanced ANXA2 expression has been correlated with angiogenesis, tumor invasion and progression in breast cancer [31,32]. Also, high ANXA2 expression has been associated with a worse survival rate in hepatocellular carcinoma [33], and an increased serum concentration of ANXA2 has been related to chemotherapy resistance in gastric cancer [34].

These evidences are representative of a biomarker with prognostic value in advanced disease. We now propose that in addition, ANXA2 may serve as therapeutic target as well as companion biomarker in the monitoring of response for its specific therapy in personalized medicine

in EC. To validate this hypothesis, we screened the Prestwick Chemical Library to identify potential hit compounds specifically targeting ANXA2, and validated Daunorubicin in model systems specifically designed to evaluate its efficacy to impair attachment of CTC to an endothelium, and prevent further metastasis both at distant and locoregional sites. Daunorubicin is an anthracycline widely used in the treatment of leukaemia. This compound exerts its cytotoxic effect by intercalating in the DNA strands, interacting with molecular oxygen to produce reactive oxygen species (ROS), inhibiting the topoisomerase II, and producing apoptosis [35,36]. The standard treatment of advanced EC is cytoreductive surgery followed by radiotherapy, chemotherapy or both. EC is a relatively chemosensitive disease being platinum-based drugs (carboplatin) and taxanes (paclitaxel) the most active agents [37]. Regarding anthracyclines, doxorubicin has also been shown to be active in EC, but presenting an unfavorable toxicity profile. The combination of cisplatin and doxorubicin showed a better response to treatment compared to doxorubicin alone but with a higher level of toxicity and no benefits in OS [38]. In addition, the comparison of carboplatin and paclitaxel *versus* the combination of doxorubicin, cisplatin, and paclitaxel chemotherapy demonstrated no difference in terms of PFS and OS but having less toxicity in the absence of doxorubicin [39]. A recent randomized study by the Japanese Gynecologic Oncology Group reached similar conclusions, with no significant difference of survival among patients receiving doxorubicin plus cisplatin, docetaxel plus cisplatin, or paclitaxel plus carboplatin as postoperative adjuvant chemotherapy for endometrial cancer [40]. Currently efforts to mitigate the doxorubicin-induced cardiotoxicity includes liposomal doxorubicin and pegylated liposomal doxorubicin (PLD) formulations [41]. PLD should be explored in phase II and phase III studies of endometrial carcinoma [42]. Regarding Daunorubicin, this anthracycline is of clinical use in acute myeloid leukemia, whose liposomal encapsulated formulation ameliorates its safety profile [43]. Some benefits have been observed in the therapeutic response of daunorubicin compared to doxorubicin including less cardiotoxicity [44,45], but more data is needed to conclude on the clinical benefit of Daunorubicin.

5. Conclusion

In conclusion, we have confirmed, in the liquid biopsy context, the clinical value of ANXA2 in advanced EC. We also functionally validated in complex *in vitro* and *in vivo* model systems that reproduce the stepwise process of dissemination and micrometastasis formation, the impact of ANXA2 on CTC attachment and homing at distant sites. And finally, we investigated through HTS the potential of ANXA2 as therapeutic target to specifically impair these critical steps of metastasis dissemination in endometrial cancer. These evidences should be now appropriately translated into the clinical setting by, for example, selecting ANXA2-overexpressing advanced EC patients' candidates to liposome formulations of daunorubicin that could maximize its therapeutic benefit while minimizing its toxicity profile.

Funding

This work was supported by grants from the Instituto de Salud Carlos III (ISCIII), grant PI17/01919 and PI20/00969, co-financed by the European Regional Development Fund (FEDER); from Fundación Científica de la Asociación Española Contra el Cáncer (AECC), Grupos Clínicos Coordinados 2018; Xunta de Galicia (ED431C 2018/21); Ministry of Economy and Competiveness (Innopharma Project) and from CIBERONC (CB16/12/00328); Carolina Herrero is supported by a predoctoral i-PFIS fellowship from Instituto de Salud Carlos III (IFI17/00047).

Author contributions

JB, AG-M, RL-L, MIL, MA and LA-A contributed to the design of the study. CH, CPM, EC and LA-A conducted animal experiments; CH, LA-A, AP-D, EmC, NF conducted the *in vitro* experiments; CH, JB, AP-D, EmC, NF, CPM, EC MA and L-AA contributed to the data analysis and interpretation. CH, JB, A P-D, MA and LA-A drafted the manuscript. CH, JB, AP-D, EmC, NF, CPM, EC, AG-M, MIL, RL-L, MA and LA-A critically revised the manuscript. All authors approved the final version of the manuscript.

Conflict of interest statement

The authors declare that they have no known competing financial interests or personal relationships that could have appeared to influence the work reported in this paper.

Acknowledgments

We would like to thank all the patients for participating in the study. The graphical abstract was produced using Servier Medical Art (https://smart.servier.com).

Disclosure

The authors declare no potential conflicts of interest in this research.

Appendix A. Supporting information

Supplementary data associated with this article can be found in the online version at doi:10.1016/j.biopha.2021.111744.

References

[1] R.L. Siegel, K.D. Miller, A. Jemal, Cancer statistics, 2020, CA Cancer J. Clin. 70 (2020) 7–30, https://doi.org/10.3322/caac.21590.
[2] A.S. Felix, T.M. Brasky, D.E. Cohn, D.G. Mutch, W.T. Creasman, P.H. Thaker, J. L. Walker, R.G. Moore, S.B. Lele, S.R. Guntupalli, L.S. Downs, C. Nagel, J. F. Boggess, M.L. Pearl, O.B. Ioffe, W. Deng, D.S. Miller, L.A. Brinton, Endometrial carcinoma recurrence according to race and ethnicity: an NRG Oncology/Gynecologic Oncology Group 210 Study, Int. J. Cancer 142 (2018) 1102–1115, https://doi.org/10.1002/ijc.31127.
[3] P. Morice, A. Leary, C. Creutzberg, N. Abu-Rustum, E. Darai, Endometrial cancer, Lancet 387 (2016) 1094–1108, https://doi.org/10.1016/S0140-6736(15)00130-0.
[4] K. Brasseur, N. Gévry, E. Asselin, Chemoresistance and targeted therapies in ovarian and endometrial cancers, Oncotarget 8 (2017) 4008–4042, https://doi.org/10.18632/oncotarget.14021.
[5] K.M. Moxley, D.S. McMeekin, Endometrial carcinoma: a review of chemotherapy, drug resistance, and the search for new agents, Oncologist 15 (2010) 1026–1033, https://doi.org/10.1634/theoncologist.2010-0087.
[6] K.H. Lu, R.R. Broaddus, Endometrial cancer, New Engl. J. Med. 383 (2020) 2053–2064, https://doi.org/10.1056/NEJMra1514010.
[7] Y.P. Geels, J.M.A. Pijnenborg, B.B.M. Gordon, M. Fogel, P. Altevogt, R. Masadah, J. Bulten, L.C. van Kempen, L.F.A.G. Massuger, L1CAM expression is related to non-endometrioid histology, and prognostic for poor outcome in endometrioid endometrial carcinoma, Pathol. Oncol. Res. 22 (2016) 863–868, https://doi.org/10.1007/s12253-016-0047-8.
[8] L.J.M. van der Putten, N.C.M. Visser, K. van de Vijver, M. Santacana, P. Bronsert, J. Bulten, M. Hirschfeld, E. Colas, A. Gil-Moreno, A. Garcia, G. Mancebo, F. Alameda, J. Trovik, R.K. Kopperud, J. Huvila, S. Schrauwen, M. Koskas, F. Walker, V. Weinberger, L. Minar, E. Jandakova, M.P.L.M. Snijders, S. van den Berg-van Erp, X. Matias-Guiu, H.B. Salvesen, H.M.J. Werner, F. Amant, L.F.A. G. Massuger, J.M.A. Pijnenborg, Added value of estrogen receptor, progesterone receptor, and L1 cell adhesion molecule expression to histology-based endometrial carcinoma recurrence prediction models: an ENITEC Collaboration Study, Int. J. Gynecol. Cancer 28 (2018) 514–523, https://doi.org/10.1097/IGC.0000000000001187.
[9] L. Alonso-Alconada, M. Santacana, P. Garcia-Sanz, L. Muinelo-Romay, E. Colas, C. Mirantes, M. Monge, J. Cueva, E. Oliva, R.A. Soslow, M.A. Lopez, J. Palacios, J. Prat, J. Valls, C. Krakstad, H. Salvesen, A. Gil-Moreno, R. Lopez-Lopez, X. Dolcet, G. Moreno-Bueno, J. Reventos, X. Matias-Guiu, M. Abal, Annexin-A2 as predictor biomarker of recurrent disease in endometrial cancer, Int. J. Cancer 136 (2015) 1863–1873, https://doi.org/10.1002/ijc.29213.
[10] C. Herrero, A. de la Fuente, C. Casas-Arozamena, V. Sebastian, M. Prieto, M. Arruebo, A. Abalo, E. Colás, G. Moreno-Bueno, A. Gil-Moreno, A. Vilar, J. Cueva, M. Abal, L. Muinelo-Romay, Extracellular vesicles-based biomarkers represent a promising liquid biopsy in endometrial cancer, Cancers 11 (2019) 2000, https://doi.org/10.3390/cancers11122000.
[11] E. Lianidou, K. Pantel, Liquid biopsies, Genes Chromosomes Cancer 58 (2019) 219–232, https://doi.org/10.1002/gcc.22695.

[12] M. Cristofanilli, G.T. Budd, M.J. Ellis, A. Stopeck, J. Matera, M.C. Miller, J. M. Reuben, G.V. Doyle, W.J. Allard, L.W.M.M. Terstappen, D.F. Hayes, Circulating tumor cells, disease progression, and survival in metastatic breast cancer, New Engl. J. Med. 351 (2004) 781–791, https://doi.org/10.1056/NEJMoa040766.

[13] F.-C. Bidard, S. Michiels, S. Riethdorf, V. Mueller, L.J. Esserman, A. Lucci, B. Naume, J. Horiguchi, R. Gisbert-Criado, S. Sleijfer, M. Toi, J.A. Garcia-Saenz, A. Hartkopf, D. Generali, F. Rothé, J. Smerage, L. Muinelo-Romay, J. Stebbing, P. Viens, M.J.M. Magbanua, C.S. Hall, O. Engebraaten, D. Takata, J. Vidal-Martínez, W. Onstenk, N. Fujisawa, E. Diaz-Rubio, F.-A. Taran, M.R. Cappelletti, M. Ignatiadis, C. Proudhon, D.M. Wolf, J.B. Bauldry, E. Borgen, R. Nagaoka, V. Carañana, J. Kraan, M. Maestro, S.Y. Brucker, K. Weber, F. Reyal, D. Amara, M. G. Karhade, R.R. Mathiesen, H. Tokiniwa, A. Llombart-Cussac, A. Meddis, P. Blanche, K. D'Hollander, P. Cottu, J.W. Park, S. Loibl, A. Latouche, J.-Y. Pierga, K. Pantel, Circulating tumor cells in breast cancer patients treated by neoadjuvant chemotherapy: a meta-analysis, J. Natl. Cancer Inst. 110 (2018) 560–567, https://doi.org/10.1093/jnci/djy018.

[14] J.S. de Bono, H.I. Scher, R.B. Montgomery, C. Parker, M.C. Miller, H. Tissing, G. V. Doyle, L.W.W.M. Terstappen, K.J. Pienta, D. Raghavan, Circulating tumor cells predict survival benefit from treatment in metastatic castration-resistant prostate cancer, Clin. Cancer Res. 14 (2008) 6302–6309, https://doi.org/10.1158/1078-0432.CCR-08-0872.

[15] S.J. Cohen, C.J.A. Punt, N. Iannotti, B.H. Saidman, K.D. Sabbath, N.Y. Gabrail, J. Picus, M. Morse, E. Mitchell, M.C. Miller, G.V. Doyle, H. Tissing, L.W.M. M. Terstappen, N.J. Meropol, Relationship of circulating tumor cells to tumor response, progression-free survival, and overall survival in patients with metastatic colorectal cancer, J. Clin. Oncol. 26 (2008) 3213–3221, https://doi.org/10.1200/JCO.2007.15.8923.

[16] A.-M. Larsson, S. Jansson, P.-O. Bendahl, C. Levin Tykjaer Jörgensen, N. Loman, C. Graffman, L. Lundgren, K. Aaltonen, L. Rydén, Longitudinal enumeration and cluster evaluation of circulating tumor cells improve prognostication for patients with newly diagnosed metastatic breast cancer in a prospective observational trial, Breast Cancer Res. 20 (2018) 48, https://doi.org/10.1186/s13058-018-0976-0.

[17] L. Muinelo-Romay, C. Casas-Arozamena, M. Abal, Liquid biopsy in endometrial cancer: new opportunities for personalized oncology, Int. J. Mol. Sci. 19 (2018), https://doi.org/10.3390/ijms19082311.

[18] L. Alonso-Alconada, L. Muinelo-Romay, K. Madissoo, A. Diaz-Lopez, C. Krakstad, J. Trovik, E. Wik, D. Hapangama, L. Coenegrachts, A. Cano, A. Gil-Moreno, L. Chiva, J. Cueva, M. Vieito, E. Ortega, J. Mariscal, E. Colas, J. Castellvi, M. Cusido, X. Dolcet, H.W. Nijman, T. Bosse, J.A. Green, A. Romano, J. Reventos, R. Lopez-Lopez, H.B. Salvesen, F. Amant, X. Matias-Guiu, G. Moreno-Bueno, M. Abal, Molecular profiling of circulating tumor cells links plasticity to the metastatic process in endometrial cancer, Mol. Cancer 13 (2014) 223, https://doi.org/10.1186/1476-4598-13-223.

[19] C. Alix-Panabières, K. Pantel, Clinical applications of circulating tumor cells and circulating tumor DNA as liquid biopsy, Cancer Discov. 6 (2016) 479–491, https://doi.org/10.1158/2159-8290.CD-15-1483.

[20] M.A. Nieto, R.Y.-J. Huang, R.A. Jackson, J.P. Thiery, EMT: 2016, Cell 166 (2016) 21–45, https://doi.org/10.1016/j.cell.2016.06.028.

[21] C.L. Chaffer, B.P. San Juan, E. Lim, R.A. Weinberg, EMT, cell plasticity and metastasis, Cancer Metastas Rev. 35 (2016) 645–654, https://doi.org/10.1007/s10555-016-9648-7.

[22] P.G. Santamaria, G. Moreno-Bueno, F. Portillo, A. Cano, EMT: present and future in clinical oncology, Mol. Oncol. 11 (2017) 718–738, https://doi.org/10.1002/1878-0261.12091.

[23] A. Kölbl, U. Jeschke, U. Andergassen, The significance of epithelial-to-mesenchymal transition for circulating tumor cells, IJMS 17 (2016) 1308, https://doi.org/10.3390/ijms17081308.

[24] C. Alix-Panabières, S. Mader, K. Pantel, Epithelial-mesenchymal plasticity in circulating tumor cells, J. Mol. Med. 95 (2017) 133–142, https://doi.org/10.1007/s00109-016-1500-6.

[25] B. Bystricky, Z. Cierna, G. Sieberova, P. Janega, M. Karaba, G. Minarik, J. Benca, T. Sedlackova, S. Jurisova, P. Gronesova, D. Pindak, J. Macuch, J. Mardiak, M. Mego, Relationship between circulating tumor cells and Annexin A2 in early breast cancer patients, Anticancer Res. 37 (2017) 2727–2734, https://doi.org/10.21873/anticanres.11624.

[26] J. Barbazán, L. Alonso-Alconada, L. Muinelo-Romay, M. Vieito, A. Abalo, M. Alonso-Nocelo, S. Candamio, E. Gallardo, B. Fernández, I. Abdulkader, M. de los Ángeles Casares, A. Gómez-Tato, R. López-López, M. Abal, Molecular characterization of circulating tumor cells in human metastatic colorectal cancer, PLoS One 7 (2012) 40476, https://doi.org/10.1371/journal.pone.0040476.

[27] J. Barbazán, L. Alonso-Alconada, N. Elkhatib, S. Geraldo, V. Gurchenkov, A. Glentis, G. van Niel, R. Palmulli, B. Fernández, P. Viaño, T. Garcia-Caballero, R. López-López, M. Abal, D.M. Vignjevic, Liver metastasis is facilitated by the adherence of circulating tumor cells to vascular fibronectin deposits, Cancer Res 77 (2017) 3431–3441, https://doi.org/10.1158/0008-5472.CAN-16-1917.

[28] M.-E. Francart, J. Lambert, A.M. Vanwynsberghe, E.W. Thompson, M. Bourcy, M. Polette, C. Gilles, Epithelial-mesenchymal plasticity and circulating tumor cells: Travel companions to metastases, Dev. Dyn. 247 (2018) 432–450, https://doi.org/10.1002/dvdy.24506.

[29] A. Bharadwaj, M. Bydoun, R. Holloway, D. Waisman, Annexin A2 heterotetramer: structure and function, Int. J. Mol. Sci. 14 (2013) 6259–6305, https://doi.org/10.3390/ijms14036259.

[30] M.C. Sharma, Annexin A2 (ANX A2): an emerging biomarker and potential therapeutic target for aggressive cancers, Int. J. Cancer 144 (2019) 2074–2081, https://doi.org/10.1002/ijc.31817.

[31] S. Maji, P. Chaudhary, I. Akopova, P.M. Nguyen, R.J. Hare, I. Gryczynski, J. K. Vishwanatha, Exosomal Annexin II promotes angiogenesis and breast cancer metastasis, Mol. Cancer Res. 15 (2017) 93–105, https://doi.org/10.1158/1541-7786.MCR-16-0163.

[32] Y.R. Jeon, S.Y. Kim, E.J. Lee, Y.N. Kim, D.-Y. Noh, S.Y. Park, A. Moon, Identification of annexin II as a novel secretory biomarker for breast cancer, Proteomics 13 (2013) 3145–3156, https://doi.org/10.1002/pmic.201300127.

[33] H. Zhang, M. Yao, W. Wu, L. Qiu, W. Sai, J. Yang, W. Zheng, J. Huang, D. Yao, Up-regulation of annexin A2 expression predicates advanced clinicopathological features and poor prognosis in hepatocellular carcinoma, Tumor Biol. 36 (2015) 9373–9383, https://doi.org/10.1007/s13277-015-3678-6.

[34] F. Tas, C. Tilgen Yasasever, S. Karabulut, D. Tastekin, D. Duranyildiz, Circulating annexin A2 as a biomarker in gastric cancer patients: correlation with clinical variables, Biomed. Pharmacother. 69 (2015) 237–241, https://doi.org/10.1016/j.biopha.2014.12.005.

[35] J.V. McGowan, R. Chung, A. Maulik, I. Piotrowska, J.M. Walker, D.M. Yellon, Anthracycline chemotherapy and cardiotoxicity, Cardiovasc. Drugs Ther. 31 (2017) 63–75, https://doi.org/10.1007/s10557-016-6711-0.

[36] H.M. Al-Aamri, H. Ku, H.R. Irving, J. Tucci, T. Meehan-Andrews, C. Bradley, Time dependent response of daunorubicin on cytotoxicity, cell cycle and DNA repair in acute lymphoblastic leukaemia, BMC Cancer 19 (2019) 179, https://doi.org/10.1186/s12885-019-5377-y.

[37] N. Colombo, C. Creutzberg, F. Amant, T. Bosse, A. González-Martín, J. Ledermann, C. Marth, R. Nout, D. Querleu, M.R. Mirza, C. Sessa, ESMO-ESGO-ESTRO consensus conference on endometrial cancer, Int. J. Gynecol. Cancer 26 (2016) 2–30, https://doi.org/10.1097/IGC.0000000000000609.

[38] J.T. Thigpen, M.F. Brady, H.D. Homesley, J. Malfetano, B. DuBeshter, R.A. Burger, S. Liao, Phase III trial of Doxorubicin with or without cisplatin in advanced endometrial carcinoma: a Gynecologic Oncology Group Study, J. Clin. Oncol. 22 (2004) 3902–3908, https://doi.org/10.1200/JCO.2004.02.088.

[39] D. Miller, V. Filiaci, G. Fleming, R. Mannel, D. Cohn, T. Matsumoto, K. Tewari, P. DiSilvestro, M. Pearl, R. Zaino, Late-Breaking Abstract 1: randomized phase III noninferiority trial of first line chemotherapy for metastatic or recurrent endometrial carcinoma: a Gynecologic Oncology Group study, Gynecol. Oncol. 125 (2012) 771, https://doi.org/10.1016/j.ygyno.2012.03.034.

[40] H. Nomura, D. Aoki, H. Michimae, M. Mizuno, H. Nakai, M. Arai, M. Sasagawa, K. Ushijima, T. Sugiyama, M. Saito, H. Tokunaga, M. Matoda, T. Nakanishi, Y. Watanabe, F. Takahashi, T. Saito, N. Yaegashi, Effect of taxane plus platinum regimens vs doxorubicin plus cisplatin as adjuvant chemotherapy for endometrial cancer at a high risk of progression, JAMA Oncol. 5 (2019) 833–840, https://doi.org/10.1001/jamaoncol.2019.0001.

[41] A. Shafei, W. El-Bakly, A. Sobhy, O. Wagdy, A. Reda, O. Aboelenin, A. Marzouk, K. El Habak, R. Mostafa, M.A. Ali, M. Ellithy, A review on the efficacy and toxicity of different doxorubicin nanoparticles for targeted therapy in metastatic breast cancer, Biomed. Pharmacother. 95 (2017) 1209–1218, https://doi.org/10.1016/j.biopha.2017.09.059.

[42] M. Goldfinger, I. Diaz, F. Muggia, Systemic treatment of endometrial cancer: what is doxorubicin's role? J. Clin. Oncol. 32 (2014) 2181–2182, https://doi.org/10.1200/JCO.2014.55.7454.

[43] H.A. Blair, Daunorubicin/cytarabine liposome: a review in acute myeloid leukaemia, Drugs 78 (2018) 1903–1910, https://doi.org/10.1007/s40265-018-1022-3.

[44] J.D. Buckley, B.C. Lampkin, M.E. Nesbit, I.D. Bernstein, S.A. Feig, J.H. Kersey, S. Piomelli, T. Kim, G.D. Hammond, Remission induction in children with acute non-lymphocytic leukemia using cytosine arabinoside and doxorubicin or daunorubicin: a report from the Childrens Cancer Study Group, Med. Pediatr. Oncol. 17 (1989) 382–390, https://doi.org/10.1002/mpo.2950170507.

[45] E.A.M. Feijen, W.M. Leisenring, K.L. Stratton, K.K. Ness, H.J.H. van der Pal, H. N. Caron, G.T. Armstrong, D.M. Green, M.M. Hudson, K.C. Oeffinger, L.L. Robison, M. Stovall, L.C.M. Kremer, E.J. Chow, Equivalence ratio for daunorubicin to doxorubicin in relation to late heart failure in survivors of childhood cancer, J. Clin. Oncol. 33 (2015) 3774–3780, https://doi.org/10.1200/JCO.2015.61.5187.